

# Structure–activity relationship and liver microsome stability studies of pyrrole necroptosis inhibitors

Xin Teng,<sup>a</sup> Heather Keys,<sup>b</sup> Junying Yuan,<sup>c</sup> Alexei Degterev<sup>b</sup> and Gregory D. Cuny<sup>a,\*</sup>

<sup>a</sup>Laboratory for Drug Discovery in Neurodegeneration, Harvard NeuroDiscovery Center,

Brigham & Women's Hospital and Harvard Medical School, 65 Landsdowne Street, Cambridge, MA 02139, USA

<sup>b</sup>Department of Biochemistry, Tufts University Medical School, 136 Harrison Avenue, Stearns 703, Boston, MA 02111, USA

<sup>c</sup>Department of Cell Biology, Harvard Medical School, 240 Longwood Avenue, Boston, MA 02115, USA

Received 6 March 2008; accepted 22 April 2008

Available online 25 April 2008

**Abstract**—Necroptosis is a regulated caspase-independent cell death pathway resulting in morphology reminiscent of passive non-regulated necrosis. Several diverse structure classes of necroptosis inhibitors have been reported to date, including a series of [1,2,3]thiadiazole benzylamide derivatives. However, initial evaluation of mouse liver microsome stability indicated that this series of compounds was rapidly degraded. A structure–activity relationship (SAR) study of the [1,2,3]thiadiazole benzylamide series revealed that increased mouse liver microsome stability and increased necroptosis inhibitory activity could be accomplished by replacement of the 4-cyclopropyl-[1,2,3]thiadiazole with a 5-cyano-1-methylpyrrole. In addition, the SAR and the cellular activity profiles, utilizing different cell types and necroptosis-inducing stimuli, of representative [1,2,3]thiadiazole and pyrrole derivatives were very similar suggesting that the two compound series inhibit necroptosis in the same manner.

© 2008 Elsevier Ltd. All rights reserved.

Necroptosis is a regulated caspase-independent cell death pathway resulting in morphological features reminiscent of passive non-regulated necrosis.<sup>1,2</sup> Necroptosis can be induced with various stimuli (e.g., TNF- $\alpha$  and Fas ligand) and in a variety of cell types (e.g., monocytes, fibroblasts, lymphocytes, macrophages, epithelial cells, and neurons). Furthermore, it may represent a significant contributor to and in some cases predominant mode of cellular demise under pathological conditions involving excessive cell stress, rapid energy loss, and massive oxidative species generation, not conducive for highly energy-dependent processes such as apoptosis. Discovery of regulated necrotic cell death mechanisms, such as necroptosis, raises the possibility of implementing novel therapeutic intervention strategies for the treatment of diseases where necrosis is known to play a prominent role, such as organ ischemia (i.e., stroke,<sup>3</sup> myocardial infarction,<sup>4</sup> and retinal ischemia<sup>5</sup>), traumatic brain injury,<sup>6</sup> liver injury,<sup>7</sup> cancer chemo/radiation therapy-induced necrosis,<sup>8</sup> acute necro-

tizing pancreatitis,<sup>9</sup> and possibly some forms of neurodegeneration.<sup>10</sup>

To date several diverse structure classes of necroptosis inhibitors have been reported, including hydantoin containing indole derivatives (i.e., **1**),<sup>11</sup> tricyclic derivatives (i.e., **2**),<sup>12</sup> substituted 3*H*-thieno[2,3-*d*]pyrimidin-4-ones (i.e., **3**),<sup>13</sup> and [1,2,3]thiadiazole benzylamides (i.e., **4**)<sup>14</sup> (Fig. 1). In addition, ( $\pm$ )-**1** and its derivatives have

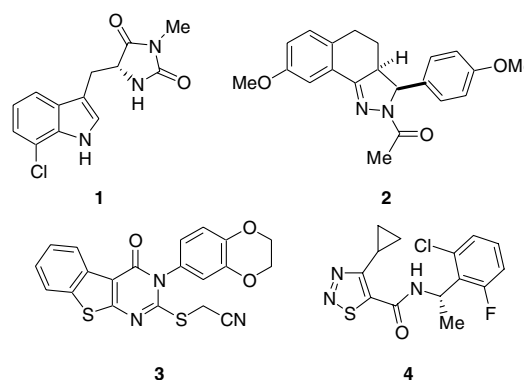


Figure 1. Necrostatins.

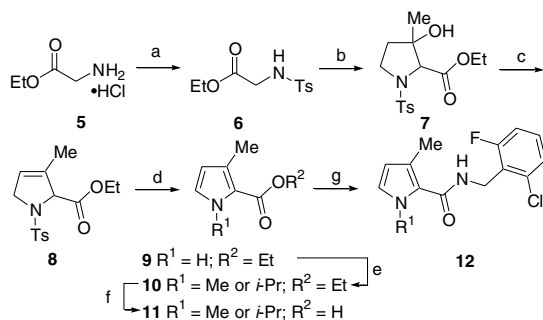
**Keywords:** Cell death; Necrosis; Necroptosis; Microsome stability; Caspase-independent; Pyrroles; SAR.

\* Corresponding author. Tel.: +1 617 768 8640; fax: +1 617 768 8606; e-mail: gcuny@rics.bwh.harvard.edu

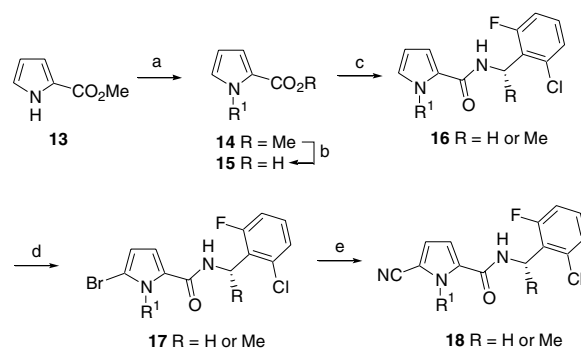
demonstrated *in vivo* activity in the temporary and permanent middle cerebral artery occlusion (MCAO) model of cerebral ischemia,<sup>1</sup> in a mouse model of ischemia/reperfusion heart injury<sup>15</sup> and in the controlled cortical impact (CCI) model of traumatic brain injury (TBI).<sup>16</sup> Structure–activity relationship (SAR) studies leading to significant potency improvements for necrostatins have been reported<sup>11–14</sup>; however, issues of bioavailability for these promising agents have not been previously addressed, except for **1**.<sup>11</sup>

In order to evaluate the *in vivo* pharmacology of other necroptosis inhibitors via preferred administration routes (i.e., oral, intravenous, intraperitoneal, or subcutaneous) they must possess adequate metabolic stability, in addition to *in vitro* potency. One efficient and cost effective method of assessing a compound's metabolic stability is to measure its resistance to metabolism over time in the presence of liver microsomes.<sup>17</sup> Utilizing this technique with mouse liver microsomes, compound **4**, which inhibits necroptosis induced with TNF- $\alpha$  in FADD-deficient variant of human Jurkat T cells with an EC<sub>50</sub> value of 0.28  $\mu$ M, demonstrated poor metabolic stability with a half-life ( $t_{1/2}$ ) of 32.5 min and intrinsic clearance (CL<sub>int</sub>) of  $42.6 \pm 3.2$   $\mu$ L/min/mg protein. Herein, we describe the results of a SAR study to optimize the mouse liver microsome stability of this inhibitor series. In addition, we evaluated the cellular activity profile of an optimized inhibitor utilizing different cell types and necroptosis-inducing stimuli.

3-Alkyl pyrrole derivatives were prepared according to the procedure outlined in Scheme 1.<sup>18</sup> Glycine ethyl ester, **5**, was treated with *p*-toluenesulfonyl chloride (Ts-Cl) to give **6**, which upon treatment with 4-diethylaminobutan-2-one in the presence of *t*-BuOK gave **7**. Dehydration with POCl<sub>3</sub> yielded the dihydropyrrole derivative **8**. Elimination in the presence of sodium ethoxide generated pyrrole derivative **9**. The pyrrole nitrogen was deprotonated with sodium hydride and alkylated to give **10**. The ester was hydrolyzed with aqueous KOH in MeOH and then the corresponding acid **11** was converted to amide **12** using EDCI.



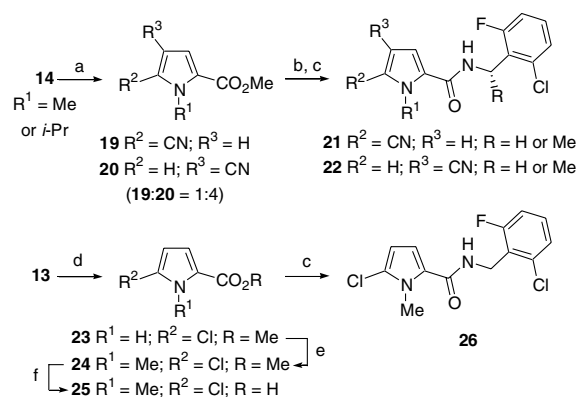
**Scheme 1.** Reagents and conditions: (a) Py, TsCl, CH<sub>2</sub>Cl<sub>2</sub>, rt, 6 h; (b) 4-diethylaminobutan-2-one, *t*-BuOK, *t*-BuOH, THF, rt, 2 days; (c) POCl<sub>3</sub>, Py, rt, 18 h, (45%, over three steps); (d) NaOEt, EtOH, rt, 5 h, (82%); (e) NaH, DMF, R<sup>1</sup>I, rt, 12 h, (60–90%); (f) KOH, MeOH, H<sub>2</sub>O, 50 °C, 12 h; (g) EDCI, HOBT, ArCH<sub>2</sub>NH<sub>2</sub>, DMF, rt, 12 h, (50–85%, over two steps).



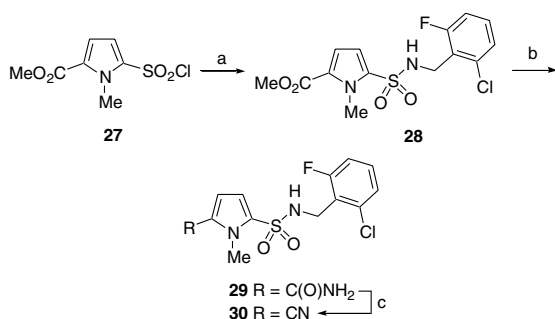
**Scheme 2.** Reagents and conditions: (a) NaH, DMF, R<sup>1</sup>I, rt, 12 h, (80–95%); (b) KOH, MeOH, H<sub>2</sub>O, rt, 8 h; (c) EDCI, HOBT, ArCH(R)NH<sub>2</sub>, DMF, rt, 12 h, (50–85%, two steps); (d) NBS, MeOH, THF, rt, 6 h, (75%); (e) Zn(CN)<sub>2</sub>, Pd(PPh<sub>3</sub>)<sub>4</sub>, DMF, 95 °C, 6 h, (85%).

1-Alkyl pyrrole derivatives were prepared according to the procedure outlined in Scheme 2. Methyl 2-pyrrole-carboxylate, **13**, was deprotonated using sodium hydride and then alkylated to give **14**. The ester was hydrolyzed to give acid **15**, which was coupled to a 2-chloro-6-fluorobenzylamine utilizing EDCI to give amide **16**. Regioselective bromination with NBS gave **17**. Finally, conversion of the aryl bromide to a nitrile was accomplished utilizing a palladium-mediated coupling with zinc cyanide to give **18** in excellent yield.<sup>19</sup>

Alternatively, cyano- and halo-substituted pyrrole derivatives were prepared according to the procedure outlined in Scheme 3. 1-Alkylpyrroles **14** were allowed to react with chlorosulfonyl isocyanate to give two readily separable regioisomeric cyanopyrrole derivatives **19** and **20** (1:4).<sup>20</sup> Each was converted to the corresponding acid and then coupled with 2-chloro-6-fluorobenzylamine to give **21** and **22**, respectively. Methyl 2-pyrrolecarboxylate, **13**, was also regioselectively chlorinated with *t*-butyl hypochlorite to give **23**.<sup>21</sup> N-alkylation gave **24** and subsequent ester hydrolysis yielded **25**, which was coupled with 2-chloro-6-fluorobenzylamine to give **26**.



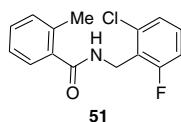
**Scheme 3.** Reagents and conditions: (a) ClSO<sub>2</sub>NCO, CH<sub>3</sub>CN, rt, 2.5 h (82%); (b) KOH, THF, MeOH, H<sub>2</sub>O, rt, 6h; (c) EDCI, HOBT, ArCH(R)NH<sub>2</sub>, DMF, rt, 12 h, (50–85%, over two steps); (d) *tert*-butyl hypochlorite, CCl<sub>4</sub>, rt, 2 days, (50%); (e) NaH, DMF, MeI, rt, 12 h, (80–95%); (f) KOH, MeOH, H<sub>2</sub>O, rt, 6 h (used without purification).



**Scheme 4.** Reagents and conditions: (a) Py, CH<sub>2</sub>Cl<sub>2</sub>, rt, 6 h, (95%); (b) 2.0 M AlMe<sub>3</sub> in hexane, NH<sub>3</sub> gas, 125 °C, PhCl, 2 days; (c) POCl<sub>3</sub>, Et<sub>3</sub>N, CHCl<sub>3</sub>, rt, 2 h (80% over two steps).

Finally, a sulfonamide pyrrole derivative was prepared according to the procedure outlined in Scheme 4. *N*-methylpyrrole sulfonyl chloride **27** was allowed to react with 2-chloro-6-fluorobenzylamine to give **28**. This material was treated with ammonia gas in the presence of trimethylaluminum to give a mixture of amide **29** and nitrile **30**.<sup>22</sup> The isolated amide **29** could be converted to nitrile **30** in the presence of phosphorous oxychloride.<sup>23</sup>

Evaluation of compounds **26**, **30**, and **31–50** (Table 1) for necroptosis inhibitory activity was performed using a FADD-deficient variant of human Jurkat T cells treated with TNF- $\alpha$  as previously described.<sup>1,12</sup> Utilizing these conditions the cells efficiently underwent necroptosis, which was completely and selectively inhibited by **1** (EC<sub>50</sub> = 0.050  $\mu$ M). For EC<sub>50</sub> value determinations, cells were treated with 10 ng/mL of human TNF- $\alpha$  in the presence of increasing concentration of test compounds for 24 h followed by ATP-based viability assessment. Microsome stability was determined in pooled mouse liver microsomes.<sup>24</sup> The results of the biological studies are shown in Table 2.



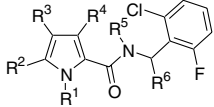
The heterocyclic ring in **4** was presumed to be most likely responsible for the compound's lack of metabolic stability. To test this hypothesis, a related derivative that replaced the 4-alkyl-[1,2,3]thiadiazole with a 2-methyl-phenyl (i.e., **51**) was prepared. This compound was devoid of necroptosis inhibitory activity, but demonstrated a significant improvement in mouse microsome stability with a  $t_{1/2}$  of 194 min and CL<sub>int</sub> of  $7.13 \pm 7.3$   $\mu$ L/min/mg protein. Based on these findings other surrogates for the [1,2,3]thiadiazole were sought that would retain necroptosis inhibitory activity.

Replacement of the 4-cyclopropyl-[1,2,3]thiadiazole with a pyrrole (**31**), a 3-alkylpyrrole (**32**), or 1,3-dialkylpyrroles (**33** and **34**) resulted in significant decreases in necroptosis inhibitory activity compared with **4**. However, replacement with 1-methyl- or 1-isopropylpyrrole

(**35** and **36**) resulted in a less significant decrease in activity suggesting that *N*-alkylpyrroles may present a possible replacement. However, **35** demonstrated poor mouse microsome stability presumably due to the electron-rich nature of the pyrrole ring. Increasing the size of the alkyl group (**37** and **38**) resulted in further decreases in necroptosis inhibitory activity. In addition, a tertiary amide (**39**) was not tolerated. This result was consistent with the SAR previously established for the [1,2,3]thiadiazole series.<sup>14</sup> Introduction of a methyl group on the benzylic position of the amide (**40**) resulted in a decrease in necroptosis inhibitory activity. However, again consistent with the SAR for the [1,2,3]thiadiazole series, all of the activity resided with the (*S*)-enantiomer (**41** vs **42**) and large substituents on the benzylic carbon (**43**) were not tolerated. Addition of electron-withdrawing groups to the 5-position of the pyrrole that would render it less electron rich was tolerated (**26** and **44**), with nitrile (**45**) being best. In the case of **26** mouse microsome stability was worst compared with **4**. However, **45** showed a slight improvement in stability. Interestingly, introduction of the nitrile to the 4-position of the pyrrole (**49** and **50**) eliminated necroptosis inhibitory activity. Increasing the size of the alkyl group on the 1-position of the pyrrole (**46** and **47**) was also detrimental to necroptosis inhibitory activity. However, introduction of a (*S*)-methyl substituent to the benzylic amide position of the 5-cyano-1-methylpyrrole (**48**)<sup>25</sup> resulted in a significant increase in *both* necroptosis inhibitory activity (EC<sub>50</sub> = 92 nM) and mouse microsome stability ( $t_{1/2}$  = 236 min and in CL<sub>int</sub> of  $5.9 \pm 2.5$   $\mu$ L/min/mg protein). Finally, sulfonamide **30** was found to be inactive as a necroptosis inhibitor further demonstrating the importance of the secondary amide functionality.

Although the precise mechanism of necroptosis inhibition by the [1,2,3]thiadiazole series is not currently known, it has shown a unique inhibitory profile compared to ( $\pm$ )-**1** and **2** when evaluated in different cell types and utilizing different necroptosis-inducing stimuli.<sup>12,14</sup> Therefore, a similar analysis was conducted comparing **48** with ( $\pm$ )-**1** and **4** (Fig. 2). The cellular activity profiles for the [1,2,3]thiadiazole and pyrrole inhibitors were very similar suggesting that the two compound series inhibit necroptosis in the same manner and that the 5-cyano-1-methylpyrrole in **48** acts as a bioisostere for the 4-cyclopropyl-[1,2,3]thiadiazole in **4**.<sup>26</sup> Furthermore, both compounds demonstrated a very different profile compared to ( $\pm$ )-**1** suggesting that they possess a distinct mode of necroptosis inhibition.

In conclusion, 5-cyano-1-methylpyrrole was found to be an excellent surrogate for the 4-cyclopropyl-[1,2,3]thiadiazole in **4** resulting in **48**, which demonstrated significantly increased necroptosis inhibitory activity and has improved mouse microsome stability. The SAR of the pyrrole derivatives for necroptosis inhibition paralleled the [1,2,3]thiadiazoles in many respects, including the requirement for a secondary amide and when a benzylic methyl was present all of the necroptosis activity resided with the (*S*)-enantiomer. Finally, cellular activity profiles of the 5-cyano-1-methylpyrrole **48** and the [1,2,3]thiadiazole **4** utilizing different cell types and nec-

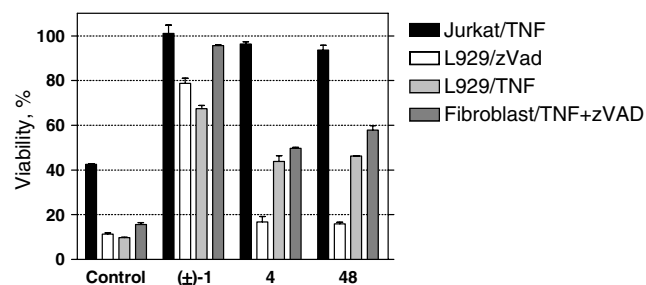
**Table 1.** Pyrrole amide derivatives prepared for inhibition of necroptosis in FADD-deficient Jurkat T cells treated with TNF- $\alpha$  and mouse microsome stability testing


Compound	R <sup>1</sup>	R <sup>2</sup>	R <sup>3</sup>	R <sup>4</sup>	R <sup>5</sup>	R <sup>6</sup>
26	Me	Cl	H	H	H	H
31	H	H	H	H	H	H
32	H	H	H	Me	H	H
33	Me	H	H	Me	H	H
34	<i>i</i> -Pr	H	H	Me	H	H
35	Me	H	H	H	H	H
36	<i>i</i> -Pr	H	H	H	H	H
37	Bn	H	H	H	H	H
38	CH(Me)Ph	H	H	H	H	H
39	Me	H	H	H	Me	H
40	<i>i</i> -Pr	H	H	H	H	( $\pm$ )-Me
41	<i>i</i> -Pr	H	H	H	H	( <i>S</i> )-Me
42	<i>i</i> -Pr	H	H	H	H	( <i>R</i> )-Me
43	<i>i</i> -Pr	H	H	H	H	( $\pm$ )- <i>n</i> -Bu
44	Et	Br	H	H	H	H
45	Me	CN	H	H	H	H
46	Et	CN	H	H	H	H
47	<i>i</i> -Pr	CN	H	H	H	H
48	Me	CN	H	H	H	( <i>S</i> )-Me
49	Me	H	CN	H	H	H
50	<i>i</i> -Pr	H	CN	H	H	H

roptosis-inducing stimuli were very similar suggesting that the two compound series inhibit necroptosis in the same manner and are distinct from **1** and **2**. Studies

**Table 2.** EC<sub>50</sub> determinations for necroptosis inhibition in FADD-deficient Jurkat T cells treated with TNF- $\alpha$  and mouse microsome stability values

Compound	EC <sub>50</sub> <sup>a</sup> ( $\mu$ M)	<i>t</i> <sub>1/2</sub> (min)	CL <sub>int</sub> ( $\mu$ L/min/mg protein)
4	0.28	32.5	42.6 $\pm$ 3.2
26	0.74	15.4	89.8 $\pm$ 3.0
30	>20	—	—
31	>20	—	—
32	4.9	—	—
33	>20	—	—
34	7.8	—	—
35	0.90	17.2	80.6 $\pm$ 4.4
36	0.44	—	—
37	>20	—	—
38	>20	—	—
39	>20	—	—
40	2.1	—	—
41	0.52	—	—
42	>20	—	—
43	>20	—	—
44	2.4	—	—
45	0.34	42.3	32.8 $\pm$ 2.2
46	1.9	—	—
47	1.4	—	—
48	0.092	236	5.9 $\pm$ 2.5
49	>20	—	—
50	>20	—	—

<sup>a</sup> Standard deviation <10%.**Figure 2.** Cell type/stimulus specific activities of necrostatins. FADD-deficient Jurkat, L929, and mouse adult lung fibroblast cells were treated for 24 h with 10 ng/mL human TNF- $\alpha$  and/or 100  $\mu$ M zVAD.fmk as indicated in the presence of 30  $\mu$ M of necrostatin ( $\pm$ )-**1**, **4**, or **48**. Cell viability was determined using an ATP-based assessment method. Values were normalized to cells treated with necrostatins in the absence of necroptotic stimulus, which were set as 100% viability. Error bars reflect standard deviation values (*N* = 2).

are currently under way to further evaluate 5-cyano-1-methylpyrrole necroptosis inhibitors in animal models of disease where necroptosis is likely to play a substantial role (i.e., liver injury) and to investigate the mechanism of necroptosis inhibition by these derivatives.

### Acknowledgments

X.T. and G.D.C. thank the Harvard NeuroDiscovery Center (HNDC) for financial support. A.D. and J.Y. thank the National Institute on Aging, National Institute of General Medical Sciences, and American Health Assistance Foundation for financial support. X.T., G.D.C., and J.Y. thank the National Institute of Neurological Disorders and Stroke (NINDS) for financial support. AD is a recipient of an NIH Mentored Scientist Development Award from the National Institute on Aging (NIA) and the Smith Family New Investigator Award from the Massachusetts Medical Foundation. We also thank Roz Southall (Cyprotex, Inc.) for assistance with the microsome stability experiments. The SV40-transformed adult mouse lung fibroblasts were a generous gift of Dr. Philip Tsichlis (Tufts University).

### References and notes

- (a) Degterev, A.; Huang, Z.; Boyce, M.; Li, Y.; Jagtap, P.; Mizushima, N.; Cuny, G. D.; Mitchison, T.; Moskowitz, M.; Yuan, J. *Nat. Chem. Biol.* **2005**, *1*, 112; (b) Cuny, G. D.; Degterev, A.; Yuan, J. *Drugs Future* **2008**, *33*, 225.
- For literature related to caspase-independent cell death see: (a) Kitanaka, C.; Kuchino, Y. *Cell Death Differ.* **1999**, *6*, 508; (b) Fiers, W.; Beyaert, R.; Declercq, W.; Vandenberghe, P. *Oncogene* **1999**, *18*, 7719; (c) Borner, C.; Monney, L. *Cell Death Differ.* **1999**, *6*, 497; (d) Edinger, A. L.; Thompson, C. B. *Curr. Opin. Cell Biol.* **2004**, *16*, 663; (e) Yu, L.; Alva, A.; Su, H.; Dutt, P.; Freundt, E.; Welsh, S.; Baehrecke, E. H.; Lenardo, M. J. *Science* **2004**, *304*, 1500; (f) Chipuk, J. E.; Green, D. R. *Nat. Rev. Mol. Cell Biol.* **2005**, *6*, 268; (g) Bröcker, L. E.; Kruyt, F. A. E.; Giaccone, G. *Clin. Cancer Res.* **2005**, *11*, 3155; (h) Fink, S. L.; Cookson, B. T. *Infect. Immun.* **2005**, *73*, 1907; (i) Kroemer, G.; Martin, S. J. *Nat. Med.* **2005**, *11*, 725; (j)

- Vandenabeele, P.; Vanden Berghe, T.; Festjens, N. *Sci. STKE* **2006**, 358, pe44; (k) Martinet, W.; Schrijvers, D. M.; Herman, A. G.; De Meyer, G. R. *Autophagy* **2006**, 2, 312.
3. Lo, E. H.; Dalkara, T.; Moskowitz, M. A. *Nat. Rev. Neurosci.* **2003**, 4, 399.
  4. McCully, J. D.; Wakiyama, H.; Hsieh, Y. J.; Jones, M.; Levitsky, S. *Am. J. Physiol. Heart Circ. Physiol.* **2004**, 286, H1923.
  5. Osborn, N. N.; Casson, R. J.; Wood, J. P.; Chidlow, G.; Graham, M.; Melena, J. *Prog. Retin. Eye Res.* **2004**, 23, 91.
  6. Gennarelli, T. A.; Graham, D. I. In *Textbook of Traumatic Brain Injury*; Silver, J. M., McAllister, T. W., Yudofsky, S. C., Eds.; American Psychiatric Publishing Inc.: Washington, DC, 2005; p 37.
  7. (a) Kaplowitz, N. *J. Hepatol.* **2000**, 32, 39; (b) Malhi, H.; Gores, G. J.; Lemasters, J. J. *Hepatology* **2006**, 43, S31; (c) Ferrell, L. D.; Theise, N. D.; Scheuer, P. J. In *Pathology of the Liver*; MacSween, R. N. M., Burt, A. D., Portmann, B. C., Ishak, K. G., Scheuer, P. J., Anthony, P. P., Eds., 4th ed.; Churchill Livingstone: London, 2002; p 314.
  8. (a) Giglio, P.; Gilbert, M. R. *Neurologist* **2003**, 9, 180; (b) Ramesh, G.; Reeves, W. B. *Am. J. Physiol. Renal Physiol.* **2003**, 285, F610; (c) Miyaguchi, M.; Takashima, H.; Kubo, T. *J. Laryngol. Otol.* **1997**, 111, 763.
  9. (a) Rosai, J., 9th ed.. In *Rosai and Ackerman's Surgical Pathology*; Mosby: New York, 2004; Vol. 1, p 1063; (b) Wroblewski, D. M.; Barth, M. M.; Oyen, L. J. *AACN Clin. Issues* **1999**, 10, 464.
  10. Martin, L. J.; Al-Abdulla, N. A.; Brambrink, A. M.; Kirsch, J. R.; Sieber, F. E.; Portera-Cailliau, C. *Brain Res. Bull.* **1998**, 46, 281.
  11. Teng, X.; Degterev, A.; Jagtap, P.; Xing, X.; Choi, S.; Denu, R.; Yuan, J.; Cuny, G. D. *Bioorg. Med. Chem. Lett.* **2005**, 15, 5039.
  12. Jagtap, P. G.; Degterev, A.; Choi, S.; Keys, H.; Yuan, J.; Cuny, G. D. *J. Med. Chem.* **2007**, 50, 1886.
  13. Wang, K.; Li, J.; Degterev, A.; Hsu, E.; Yuan, J.; Yuan, C. *Bioorg. Med. Chem. Lett.* **2007**, 17, 1455.
  14. Teng, X.; Keys, H.; Jeevanandam, A.; Porco, J. A., Jr.; Degterev, A.; Yuan, J.; Cuny, G. D. *Bioorg. Med. Chem. Lett.* **2007**, 17, 6836.
  15. Smith, C. C. T.; Davidson, S. M.; Lim, S. Y.; Simpkin, J. C.; Hothersall, J. S.; Yellon, D. M. *Cardiovasc. Drugs Ther.* **2007**, 21, 227.
  16. You, Z.; Savitz, S. I.; Yang, J.; Degterev, A.; Yuan, J.; Cuny, G. D.; Moskowitz, M. A.; Whalen, M. J. *J. Cereb. Blood Flow Metab.*, submitted for publication.
  17. Baranczewski, P.; Stańczak, A.; Sundberg, K.; Svensson, R.; Wallin, A.; Jansson, J.; Garberg, P.; Postlind, H. *Pharmacol. Rep.* **2006**, 58, 453.
  18. Terry, W. G.; Jackson, A. H.; Kenner, G. W.; Kornis, G. *J. Chem. Soc.* **1965**, 4389.
  19. Burgey, C. S.; Robinson, K. A.; Lyle, T. A.; Sanderson, P. E. J.; Lewis, S. D.; Lucas, B. J.; Krueger, J. A.; Singh, R.; Miller-Stein, C.; White, R. B.; Wong, B.; Lyle, E. A.; Williams, P. D.; Coburn, C. A.; Dorsey, B. D.; Barrow, J. C.; Stranieri, M. T.; Holahan, M. A.; Sitko, G. R.; Cook, J. J.; McMasters, D. R.; McDonough, C. M.; Sanders, W. M.; Wallace, A. A.; Clayton, F. C.; Bohn, D.; Leonard, Y. M.; Detwiler, T. J., Jr.; Lynch, J. J., Jr.; Yan, Y.; Chen, Z.; Kuo, L.; Gardell, S. J.; Shafer, J. A.; Vacca, J. P. *J. Med. Chem.* **2003**, 46, 461.
  20. Loader, C. E.; Anderson, H. J. *Can. J. Chem.* **1981**, 59, 2673.
  21. Kim, K. S.; Lu, S.; Cornelius, L. A.; Lombardo, L. J.; Borzilleri, R. M.; Schroeder, G. M.; Sheng, C.; Rovnyak, G.; Crews, D.; Schmidt, R. J.; Williams, D. K.; Bhide, R. S.; Traeger, S. C.; McDonnell, P. A.; Mueller, L.; Sheriff, S.; Newitt, J. A.; Pudzianowski, A. T.; Yang, Z.; Wild, R.; Lee, F. Y.; Batorsky, R.; Ryder, J. S.; Ortega-Nanos, M.; Shen, H.; Gottardis, M.; Roussell, D. L. *Bioorg. Med. Chem. Lett.* **2006**, 16, 3937.
  22. Li, X.; Reuman, M.; Russell, R. K. *Heterocycles* **2006**, 70, 201.
  23. Kini, G. D.; Robins, R. K.; Avery, T. L. *J. Med. Chem.* **1989**, 32, 1447.
  24. Microsome stability was determined in pooled mouse liver microsomes. Test compound (3  $\mu$ M final concentration) along with 0.5 mg/mL microsome protein and 1 mM NADPH was incubated for 0, 5, 15, 30, and 60 min. Incubation of test compound and microsomes in the absence of NADPH served as a negative control. The samples were quenched with methanol and centrifuged for 20 min at 2500 rpm to precipitate proteins. Sample supernatants were analyzed ( $N = 3$ ) by LC/MS. The  $\ln$  peak area ratio (compound peak area/internal standard peak area) was plotted against time and the slope of the line determined to give the elimination rate constant [ $k = (-1)(\text{slope})$ ]. The half-life ( $t_{1/2}$  in minutes) and the in vitro intrinsic clearance ( $\text{CL}_{\text{int}}$  in  $\mu\text{L}/\text{min}/\text{mg}$  protein) were calculated according to the following equations, where  $V$  = incubation volume in  $\mu\text{L}/\text{mg}$  protein:
 
$$t_{1/2} = \frac{0.693}{k}; \quad \text{CL}_{\text{int}} = \frac{V(0.693)}{t_{1/2}}.$$
  25. **Compound 48**:  $^1\text{H}$  NMR (400 MHz,  $\text{CDCl}_3$ ):  $\delta$  7.23–7.15 (m, 2H), 7.05–6.97 (m, 1H), 6.79 (d, 1H,  $J = 8.8$  Hz), 6.73 (d, 1H,  $J = 4.4$  Hz), 6.54 (d, 1H,  $J = 4.4$  Hz), 5.95–5.84 (m, 1H), 4.03 (s, 3H), 1.59 (d, 3H,  $J = 7.2$  Hz);  $^{13}\text{C}$  NMR (100 MHz,  $\text{CDCl}_3$ ):  $\delta$  163.0, 160.5, 159.4, 133.8, 133.7, 130.5, 129.3, 129.2, 128.5, 128.4, 126.3, 118.2, 115.2, 115.0, 113.0, 111.4, 109.8, 43.9, 35.3, 20.4; HRMS Calculated for  $\text{C}_{15}\text{H}_{14}\text{ClFN}_3\text{O}$   $[\text{M}+\text{H}]^+$  306.0809. Found: 306.0804.
  26. (a) Chen, X.; Wang, W. *Ann. Rep. Med. Chem.* **2003**, 38, 333; (b) Olesen, P. H. *Curr. Opin. Drug Discov. Dev.* **2001**, 4, 471.